Propulsion and Power Research 2016;5(2):164–175

HOSTED BY

ELSEVIER

http://ppr.buaa.edu.cn/

Propulsion and Power Research

www.sciencedirect.com

ORIGINAL ARTICLE

The effect of induced magnetic field and convective boundary condition on MHD stagnation point flow and heat transfer of upper-convected Maxwell fluid in the presence of nanoparticle past a stretching sheet

Wubshet Ibrahim*

Department of Mathematics, Ambo University, P.O. Box 19, Ambo, Ethiopia

Received 5 February 2015; accepted 17 July 2015
Available online 30 May 2016

KEYWORDS

Nanofluid;
Stagnation point flow;
Heat transfer;
Convective boundary condition;
Induced magnetic field;
Upper-convected Maxwell fluid

Abstract The present study examines the effect of induced magnetic field and convective boundary condition on magnetohydrodynamic (MHD) stagnation point flow and heat transfer due to upper-convected Maxwell fluid over a stretching sheet in the presence of nanoparticles. Boundary layer theory is used to simplify the equation of motion, induced magnetic field, energy and concentration which results in four coupled non-linear ordinary differential equations. The study takes into account the effect of Brownian motion and thermophoresis parameters. The governing equations and their associated boundary conditions are initially cast into dimensionless form by similarity variables. The resulting system of equations is then solved numerically using fourth order Runge-Kutta-Fehlberg method along with shooting technique. The solution for the governing equations depends on parameters such as, magnetic, velocity ratio parameter B, Biot number Bi, Prandtl number Pr, Lewis number Le, Brownian motion Nb, reciprocal of magnetic Prandtl number A, the thermophoresis parameter Nt, and Maxwell parameter β.

The numerical results are obtained for velocity, temperature, induced magnetic field and concentration profiles as well as skin friction coefficient, the local Nusselt number and Sherwood number. The results indicate that the skin friction coefficient, the local Nusselt number and Sherwood number decrease with an increase in B and M parameters. Moreover, local Sherwood number $-\phi'(0)$ decreases with an increase in convective parameter Bi, but the

*Tel.: +251 911892494.
E-mail address: wubshetib@yahoo.com

Peer review under responsibility of National Laboratory for Aeronautics and Astronautics, China.

http://dx.doi.org/10.1016/j.jppr.2016.05.003

local Nusselt number $-\theta'(0)$ increases with an increase in *Bi*. The results are displayed both in graphical and tabular form to illustrate the effect of the governing parameters on the dimensionless velocity, induced magnetic field, temperature and concentration. The numerical results are compared and found to be in good agreement with the previously published results on special cases of the problem.

1. Introduction

The study of MHD stagnation point flow of a viscous incompressible fluid over a stretching sheet has attracted the interest of many researchers due to its important applications in industry and manufacturing processing [1–6]. Particularly, the study of steady magnetohyderodynamic (MHD) stagnation point flow of an electrically fluid has numerous applications. Some of which are found in the field of metallurgy and chemical engineering process such as, drawing, annealing and thinning of copper wire, etc.

Magnetic field is one of the important factors by which the cooling rate can be controlled and the desired quality of the industrial product can be achieved. Many investigations were made to examine flow characteristics over a stretching sheet under different conditions of MHD. Concerning this, Pavlov [7] and Hayat et al. [8] have investigated the effect of a magnetic field on the viscous flow of an electrically conducting fluid past a stretching sheet.

The study of MHD boundary layer flow over a stretching sheet has extended and included other parameters, such as induced magnetic field. Accordingly, Ali et al. [9] examined MHD boundary layer flow and heat transfer over a stretching sheet with induced magnetic field. The result shows that the velocity and the induced magnetic field profiles increase with an increase in the applied magnetic field. Furthermore, they discussed some important application areas of MHD flow, such as in designating cooling system with liquid metals, MHD generator and other devices in many manufacturing industries.

Ali et al. [10] also studied the effect of induced magnetic field on the stagnation point flow of Newtonian fluids. The numerical results of their study indicated that the skin friction coefficient decreases as the magnetic parameter increases. Furthermore, Ali et al. [11] studied numerically the MHD mixed convection boundary layer flow towards a stagnation point flow on a vertical surface with the effect of induced magnetic field. It is indicated that the induced field is most affected by the reciprocal of the magnetic Prandtl number when compared with the skin friction and heat transfer coefficients. Still further, Kumari and Nath [12] analyzed numerically steady mixed convection stagnation point flow upper convected Maxwell fluids with induced magnetic field. Their study shows that the surface velocity gradient and heat transfer are increased by increasing magnetic and buoyancy parameters.

Recently, the study of heat transfer under convective boundary condition received numerous interests on the researcher's side due to its influence on heat transfer characteristics on the surface and consequently, the quality of the final product of the manufacturing industries. The study of a convective heat transfer in magnetic field is important in processes, such as gas turbine, nuclear plants, thermal energy storage, etc. Aziz [13] was a pioneer in using convective heating process to study boundary layer flow of the classical Blasius problem over a flat plate. He studied a similarity solution for laminar thermal boundary layer flow over a flat plate with convective boundary condition. Furthermore, Aziz [14] continued his investigation on flat plate with convective boundary condition and analyzed hydrodynamic and thermal slip flow boundary layer over a flat plate with constant heat flux boundary condition. Since then, different researchers extended the idea to various configurations of the flat plate and stretching sheet. Accordingly, researchers in the references [15–19] studied the heat transfer under convective boundary condition over a surface.

Furthermore, Makinde and Olanrewaju [20] studied the combined effects of buoyancy force and convective heat transfer on thermal boundary layer over a vertical plate with convective boundary condition. Still further, investigators in refs. [21–22] studied the convective heating condition by taking into account the condition, such as slip, permeability, porosity for Newtonian and non-Newtonian fluids over a surface.

Nowadays, the studies on boundary layer flow and heat transfer of a nanofluid is active research area in fluid science and engineering, and many research papers have been published on this area. Moreover, investigators in the references [23–27] have studied the convective boundary-layer flow of a nanofluid past a stretching surface. They used the model in which Brownian motion and thermophoresis effects were taken into account. Their result indicates that the local Nusselt number is a decreasing function of the parameters, such as Brownian motion and thermophoresis parameter.

Furthermore, Olanrewaju and Makinde [28] have analyzed a boundary layer stagnation point flow of a nanofluid over a permeable flat surface with Newtonian heating. Still further, Wubshet and Shanker [29] have numerically examined the boundary-layer flow and heat transfer of

Nomenclature

A	the reciprocal of the magnetic Prandtl number
B	velocity ratio
Bi	Biot number
B_0	magnetic field parameter
C_f	skin friction coefficient
C_∞	ambient concentration
D_B	Brownian diffusion coefficient
D_T	thermophoresis diffusion coefficient
f	dimensionless velocity stream function
h	dimensionless magnetic stream function
h_f	heat transfer coefficient
k	thermal conductivity
Le	Lewis number
M	magnetic parameter
Nb	Brownian motion parameter
Nt	theromophoresis parameter
Nu_x	local Nusselt number
Pr	Prandtl number
Re_x	local Reynolds number
Sh_x	local Sherwood number
T	temperature of the fluid inside the boundary layer
T_w	uniform temperature over the surface of a sheet
T_f	temperature of hot fluid
T_∞	ambient temperature
u, v	velocity component along x and y direction

Greek letters

α	thermal diffusivity
β	Deborah number
η	dimensionless similarity variable
μ	dynamic viscosity of the fluid
υ	kinematic viscosity of the fluid
ψ	stream function
θ	dimensionless temperature
τ	parameter defined by $(\rho c)_p/(\rho c)_f$
σ	electrical conductivity

Subscripts

∞	condition at the free stream
w	condition at the surface

Nanofluid over a vertical plate with convective surface boundary condition. Their study indicated that the local Nusselt number and Sherwood number increase with an increase in convective parameter and Lewis number. Still further, Khan and Reddy [30] have conducted a numerical study of boundary layer flow of a power-law nanofluid past a non-isothermal stretching wall with convective surface boundary condition. The results show that the skin friction is higher for pseudo plastic fluids than dilatant fluids. Vajravelu et al. [31] have also discussed the convective heat transfer in a nanofluid flow over a stretching surface by focusing on Ag-water and Cu-water nanofluid. They have investigated the effects of the nanoparticle volume fraction on the flow and heat transfer characteristics under the influence of thermal buoyancy and temperature dependent internal heat generation or absorption. Their numerical result indicates that an increase in the nanoparticle volume fraction will decrease the velocity boundary layer thickness while increasing the thermal boundary layer thickness. Moreover, Mustafa et al. [32] and Bachok et al. [33] have studied the stagnation point flow and heat transfer characteristic of a nanofluid over a stretching sheet. Their findings show that the highest value of heat transfer was obtained for Cu nanoparticle near the nodal point. Furthermore, Wubshet et al. [34] investigated the MHD stagnation point flow and heat transfer due to nanofluid towards a stretching sheet numerically. Their analysis indicates that an increase in velocity ratio parameter A increases both the local Nusslet number and local Sherwood number. Wubshet and Shanker [35] also have analyzed MHD boundary layer flow and heat transfer of a nanofluid past a permeable stretching sheet with velocity, thermal and solutal slip boundary conditions. Moreover, Wubshet and Makinde [36] studied the effect of double stratification on boundary layer flow and heat transfer of nanofluid over a vertical plate and Wubshet and Shankar [37] have examined magnetohydrodynamic boundary layer flow and heat transfer of a nanofluid over non-isothermal stretching sheet. More studies on nanofluid boundary layer are given in the references [38–47].

From the examined literature, the problem of the effect of induced magnetic on a boundary layer flow of MHD Stagnation point flow and heat transfer of upper-convected Maxwell fluid in the presence of nanoparticles has not been discussed so far. In view of this, the authors, in the present paper aim to analyze the effect of induced magnetic and convective heating on MHD stagnation point flow, the boundary layer flow and heat transfer of upper-convected Maxwell fluid with nanoparticle over a stretching sheet using Runge-Kutta-Fehlberg method with shooting technique. The effects of governing parameters on fluid velocity, induced magnetic field, temperature and particle concentration have been discussed and shown graphically and in tables. The results are compared with the results available in the literature and are found to be in an excellent agreement.

2. Mathematical formulation

Consider a two-dimensional steady state MHD stagnation point boundary layer flow and heat transfer of upper-convected Maxwell fluid over stretching sheet in the presence of nanoparticles. The flow is subjected to a convective heating process at its lower surface, which is characterized by a temperature T_f and a heat transfer coefficient h_f. Moreover, the effect of induced magnetic

field is taken into account. The coordinate system chosen in such way that the x-axis is along the sheet and y-axis is normal to the sheet. At this boundary, concentration C takes constant value C_w. The ambient value attained as y tends to infinity of T and C are denoted by T_∞ and C_∞, respectively. The free stream velocity is assumed to be in the form $u_\infty = bx$ and the velocity of the stretching sheet is $u_w = ax$, where a and b are positive constants. It is also assumed that a uniform induced magnetic field of strength H_0 is applied in the normal direction to the surface, while the normal component of the induced magnetic field H_2 vanishes when it reaches the surface and the parallel component H_1 approaches the value of H_0. Under these assumptions, along with the boundary-layer approximations, the governing equation of mass, momentum, thermal energy and concentration of steady, laminar boundary-layer flow of a nanofluid past a stretching sheet is given by Kumari and Nath [12] as:

$$\frac{\partial u}{\partial x}+\frac{\partial v}{\partial y}=0 \tag{1}$$

$$\frac{\partial H_1}{\partial x}+\frac{\partial H_2}{\partial y}=0 \tag{2}$$

$$\begin{aligned} u\frac{\partial u}{\partial x}+v\frac{\partial u}{\partial y} &= -\lambda\left(u^2\frac{\partial^2 u}{\partial x^2}+v^2\frac{\partial^2 u}{\partial y^2}+2uv\frac{\partial^2 u}{\partial x\partial y}\right) \\ &+\upsilon\frac{\partial^2 u}{\partial y^2}+u_\infty\frac{\partial u_\infty}{\partial x}+\frac{\sigma B_0^2}{\rho_f}(u_\infty-u) \\ &+\frac{\mu}{4\pi\rho_f}\left(H_1\frac{\partial H_1}{\partial x}+H_2\frac{\partial H_1}{\partial y}\right)-\frac{\mu}{4\pi\rho_f}H_e\frac{\partial H_e}{\partial x} \end{aligned} \tag{3}$$

$$u\frac{\partial H_1}{\partial x}+v\frac{\partial H_1}{\partial y}=H_1\frac{\partial u}{\partial x}+H_2\frac{\partial u}{\partial y}+\mu_e\frac{\partial^2 H_1}{\partial y^2} \tag{4}$$

$$u\frac{\partial T}{\partial x}+v\frac{\partial T}{\partial y}=\alpha\frac{\partial^2 T}{\partial y^2}+\tau\left\{D_B\frac{\partial c}{\partial y}\frac{\partial T}{\partial y}+\frac{D_T}{T_\infty}\left(\frac{\partial T}{\partial y}\right)^2\right\} \tag{5}$$

$$u\frac{\partial C}{\partial x}+v\frac{\partial C}{\partial y}=D_B\frac{\partial^2 C}{\partial y^2}+\frac{D_T}{T_\infty}\frac{\partial^2 T}{\partial y^2} \tag{6}$$

The boundary conditions are:

where

$$\begin{aligned} &\alpha=\frac{k}{(\rho c)_f}, \quad \tau=\frac{(\rho c)_p}{(\rho c)_f} \\ &u=u_w=ax, \quad v=0, \quad \frac{\partial H_1}{\partial y}=H_2=0, \\ &-k\frac{\partial T}{\partial y}=h_f(T_f-T), \quad C=C_w \quad \text{at} \quad y=0 \\ &u\to u_\infty=bx, \quad v=0, \quad H_1=H_e(x)\to H_0(x), \\ &T\to T_\infty, \quad C\to C_\infty \ \text{ as } \ y\to\infty \end{aligned} \tag{7}$$

Where k is the thermal conductivity of the fluid, H_1 and H_2 are the magnetic components along x and y, $H_e(x)$ is the x-magnetic field at the edge of the boundary layer.

The mathematical analysis of the problem is simplified by introducing the following similarity transformation.

$$\begin{aligned} &\eta=y\sqrt{\frac{a}{\upsilon}}, \quad \psi=\sqrt{a\upsilon}xf(\eta), \quad H_1=H_0xh'(\eta), \\ &H_2=-H_0\sqrt{\frac{\upsilon}{a}}h(\eta), \quad \theta(\eta)=\frac{T-T_\infty}{T_f-T_\infty}, \quad \phi(\eta)=\frac{C-C_\infty}{C_w-C_\infty} \end{aligned} \tag{8}$$

The equation of continuity is satisfied if we choose a stream function $\psi(x,y)$ such that

$$u=\frac{\partial\psi}{\partial y}, \quad v=-\frac{\partial\psi}{\partial x} \tag{9}$$

Using the similarity transformation quantities Eq. (8), the governing equations Eqs. ((1)–(6)) are transformed into the non-dimensional form as follows:

$$\begin{aligned} &f'''+ff''-f'^2+B^2+M(h'^2-hh''-1) \\ &\quad+\beta(2ff'f''-f^2f'')=0 \end{aligned} \tag{10}$$

$$Ah'''+fh''-hf''=0 \tag{11}$$

$$\theta''+Pr(f\theta'+Nb\phi'\theta'+Nt\theta'^2)=0 \tag{12}$$

$$\phi''+PrLef\phi'+\frac{Nt}{Nb}\theta''=0 \tag{13}$$

The boundary conditions are:

$$\begin{aligned} &f(0)=1, \quad f'(0)=1, \quad h(0)=h''(0)=0, \\ &\theta'(0)=-Bi(1-\theta(0)), \quad \phi(0)=1, \quad \text{at} \quad \eta=0, \\ &f'(\infty)\to B, \quad h'(\infty)\to 1, \quad \theta(\infty)\to 0, \\ &\phi(\infty)\to 0, \quad \text{as} \quad \eta\to\infty \end{aligned} \tag{14}$$

Where the governing parameter as:

$$\begin{aligned} &M=\frac{\mu}{4\pi\rho_f}\left(\frac{H_0}{a}\right)^2, \quad Bi=\frac{h_f}{k}\sqrt{\frac{\upsilon}{a}}, \quad Le=\frac{\alpha}{D_B} \\ &Nb=\frac{(\rho c)_p D_B(\phi_w-\phi_\infty)}{(\rho c)_f\alpha}, \quad \beta=\lambda a, \quad A=\frac{\mu_e}{\upsilon} \\ &Nt=\frac{(\rho c)_p D_T(T_w-T_\infty)}{(\rho c)_f\alpha T_\infty}, \quad Pr=\frac{\upsilon}{\alpha}, \quad B=\frac{b}{a} \end{aligned} \tag{15}$$

where f', h', θ and ϕ are the dimensionless velocity, induced magnetic field, temperature, and concentration respectively. f and h are the dimensionless velocity stream function and magnetic stream function, respectively, η is the similarity variable, the prime denotes differentiation with respect to η. B (velocity ratio), Pr (Prandtl number), Nb (Brownian motion parameter), Nt (thermophoresis parameter), Le (Lewis number), Bi (Biot number), β (Deborah number), M (magnetic parameter) and A is the reciprocal magnetic Prandtl number.

The magnetic parameter M, which gives the order of the ratio of the magnetic energy and the kinetic energy per unit

volume, is related to the Hartmann number Ha and the flow and magnetic Reynolds numbers Re and Re_m, respectively, as given by Ref. [10]

$$M = \frac{Ha^2}{ReRe_m}, \quad Ha = \mu H_0 \iota \left(\frac{\sigma}{\mu}\right)^{1/2}$$
$$Re = \frac{c\iota}{\upsilon}, \quad Re_m = 4\pi u_\infty \iota \mu\sigma = \frac{(c\iota)\iota}{\mu_e}$$

where ι is the characteristics length of the stretching surface comparable with the dimension of the field.

If magnetic, Deborah number and free stream velocity parameters are neglected, the problem is reduced to boundary layer flow of nanofluid past stretching sheet with convective boundary condition which was investigated by Makinde and Aziz [27].

The important physical quantities of interest in this problem are the skin friction coefficient C_f, the local Nusselt number Nu_x and the local Sherwood number Sh_x are defined as:

$$C_f = \frac{\tau_w}{\rho u_w^2}, \quad Nu_x = \frac{xq_w}{k(T_w - T_\infty)},$$
$$Sh_x = \frac{xh_m}{D_B(\phi_w - \phi_\infty)} \tag{16}$$

where the wall shear stress τ_w, the wall heat flux q_w and wall mass flux h_m are given by

$$\tau_w = \mu(1+\beta)\frac{\partial u}{\partial y}, \quad q_w = -k\left(\frac{\partial T}{\partial y}\right)_{y=0},$$
$$h_m = -D_B\left(\frac{\partial \phi}{\partial y}\right)_{y=0} \tag{17}$$

By using the above equations, we get

$$C_f\sqrt{Re_x} = (1+\beta)f''(0),$$
$$\frac{Nu_x}{\sqrt{Re_x}} = -\theta'(0), \quad \frac{Sh_x}{\sqrt{Re_x}} = -\phi'(0)$$

where Re_x, Nu_x, Sh_x are local Reynolds number, local Nusselt number and local Sherwood number, respectively.

3. Numerical solution

The transformed coupled ordinary differential equations Eqs. (10)–(13) subjected to the boundary conditions, Eq. (14) for different values of governing parameters viz. Biot number, magnetic parameter M, Prandtl number Pr,

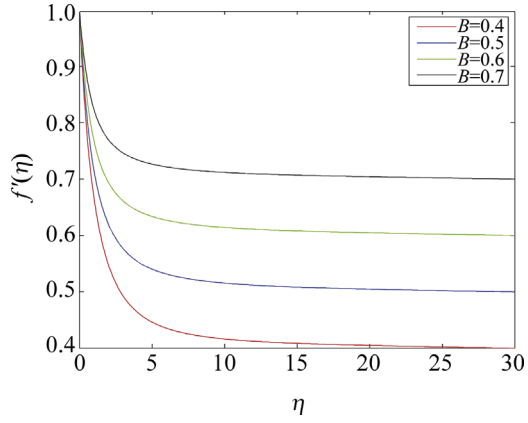

Figure 1 Velocity graph for different values of velocity ratio B when $Nb=Nt=0.1$, $Pr=0.72$, $A=0.4$, $Bi=0.5$, $Le=\beta=2$.

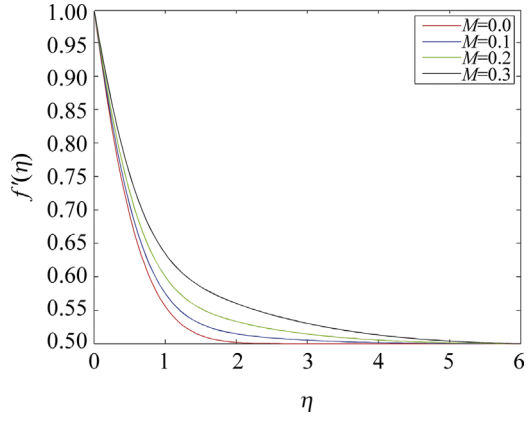

Figure 2 Velocity graph for different values of magnetic parameter M when $Nb=Nt=0.1$, $\beta=Le=A=2$, $Pr=0.72$, $B=Bi=0.5$.

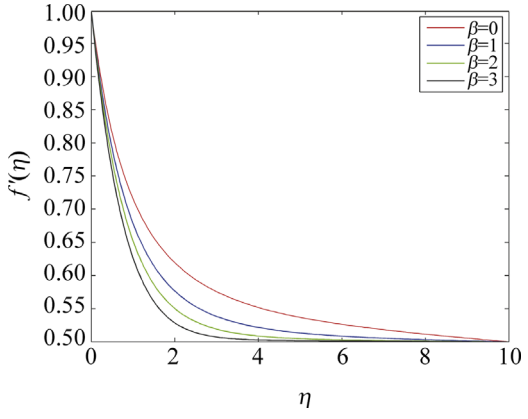

Figure 3 Velocity graph for different values of Maxwell parameter β when $Nb=Nt=0.1$, $Le=A=2$, $Pr=0.72$, $Bi=0.5$, $M=0.1$.

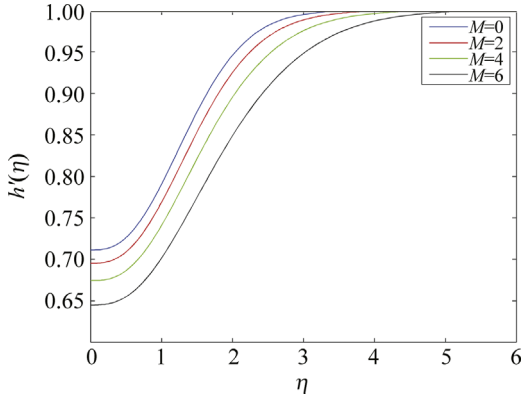

Figure 4 Induced magnetic field $h'(\eta)$ graph for different values of M when $\beta=Nb=Nt=0.1$, $Le=A=2$, $Pr=0.72$, $Bi=0.5$, $B=3$.

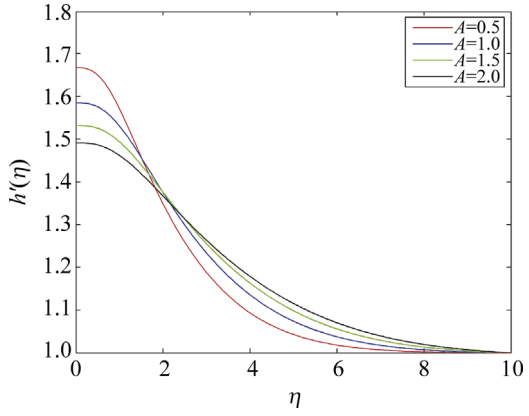

Figure 5 Induced magnetic field $h'(\eta)$ graph for different values of A when $\beta=Nb=Nt=0.1$, $Le=2$, $Pr=0.72$, $Bi=B=0.5$, $M=0.2$.

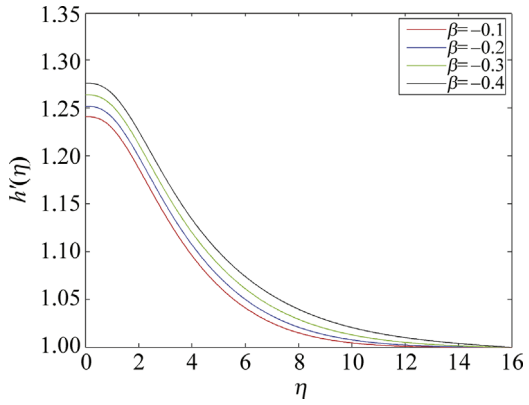

Figure 6 Induced magnetic field $h'(\eta)$ graph for different values of β when $Nb=Nt=0.1$, $Le=2$, $Pr=0.72$, $Bi=0.5$, $M=0.2$, $B=0.6$, $A=4$.

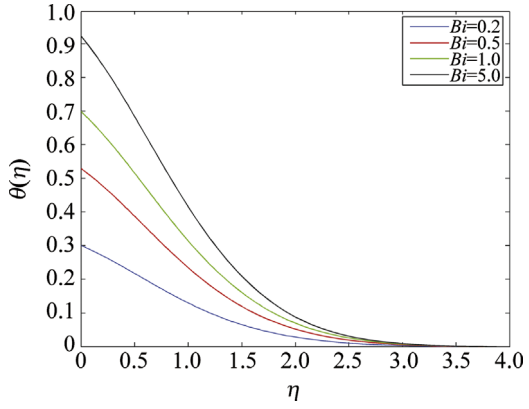

Figure 7 Temperature graph for different values of Bi when $Nb=Nt=B=M=0.5$, $Pr=1$, $Le=5$, $A=4$, $\beta=0.1$.

velocity ratio parameter B, Brownian motion parameter Nb, thermophoresis parameter Nt, Lewis number Le and β (Deborah number), has been numerically solved using Maple 17.0. This software uses a fourth-fifth order Runge-Kutta-Fehlberg method as the default method to

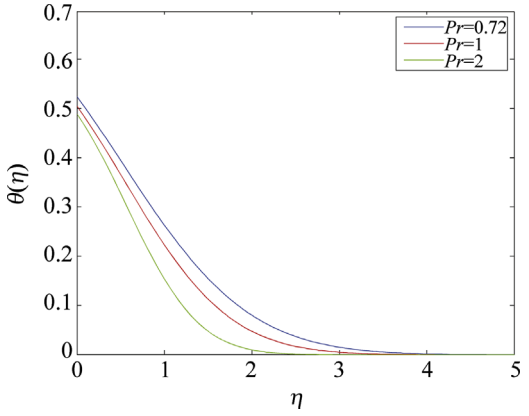

Figure 8 Temperature graph for different values of Pr when $Nb=Nt=Bi=B=M=0.5$, $Le=2$, $A=200$, $\beta=0.1$.

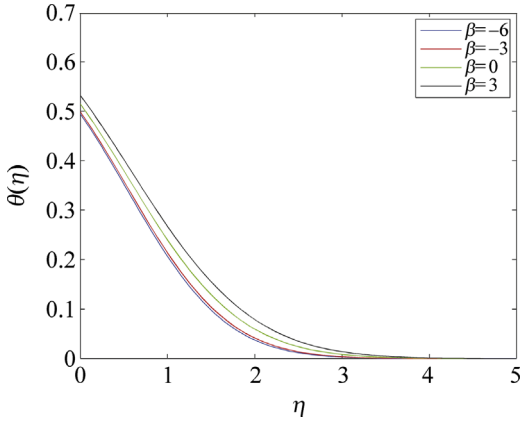

Figure 9 Temperature graph for different values of β when $Nb=Nt=Bi=0.5$, $M=0.2$, $Le=5$, $A=4$, $B=0.2$, $Pr=1$.

solve the boundary value problems numerically. Its accuracy and robustness have been confirmed by different investigators. As a further check on the accuracy of our numerical computations, it has been compared these results with the investigators [2,3,9,10] and have found to be in an excellent agreement.

4. Result and discussion

The transformed momentum, energy and concentration Eqs. (10)–(13) subjected to the boundary conditions Eq. (14) are coupled non-linear differential equation for which closed form solution can't be obtained and hence it has been solved numerically. The results are obtained for velocity, induced magnetic field, temperature, and concentration profile for different values of governing parameters. The results are displayed through Figures 1–15 for velocity, induced magnetic field, temperature, and concentration profile respectively.

Moreover, Figures 16–18 display the graph of skin friction coefficient, local Nusselt number and local Sherwood number, respectively.

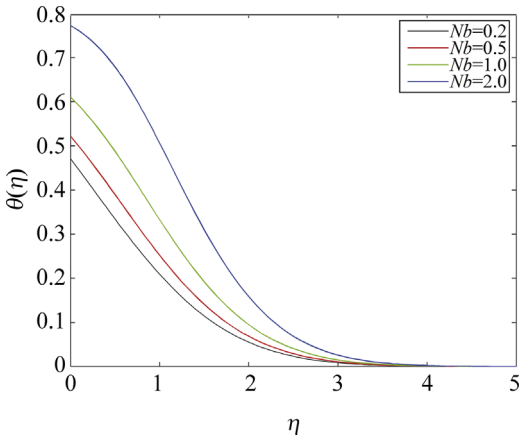

Figure 10 Temperature graph for different values of Nb when $Nt=B=Bi=0.5$, $Le=2$, $Pr=Bi=2$, $A=4$, $M=0.2$, $\beta=1$.

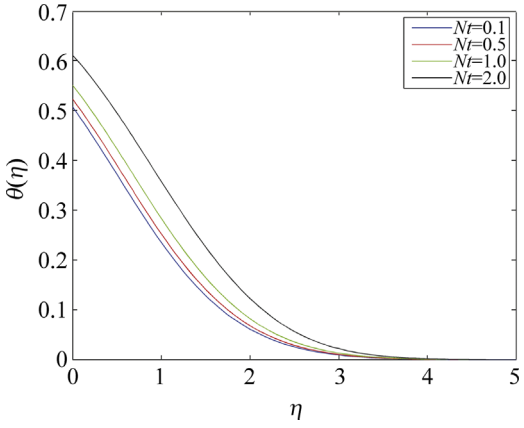

Figure 11 Temperature graph for different values of Nt when $B=Bi=Nb=0.5$, $Le=3$, $Pr=1$, $A=4$, $M=0.2$, $\beta=1$.

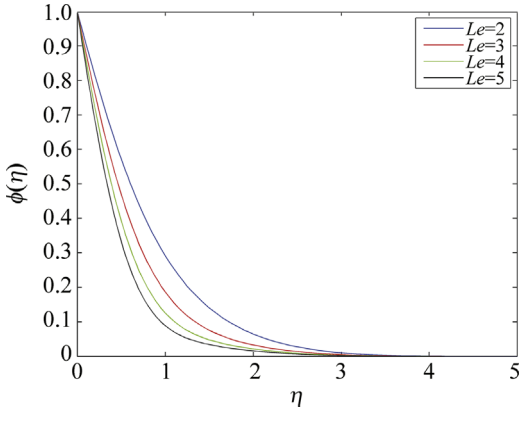

Figure 12 Concentration graph for different values of Le when $b=Nt=Bi=B=0.5$, $A=4$, $Pr=1$, $M=0.2$, $\beta=1$.

Figures 1–3 show the velocity graphs for different values of B, M and β, respectively, while the other parameters remain fixed. Figure 1 reveals the variation of velocity graph with respect to velocity ratio parameter B. As the values of B increase, the velocity boundary layer thickness increases. Besides, the graph reveals that the influence of B is more noticeable when the distance from the sheet surface is far away.

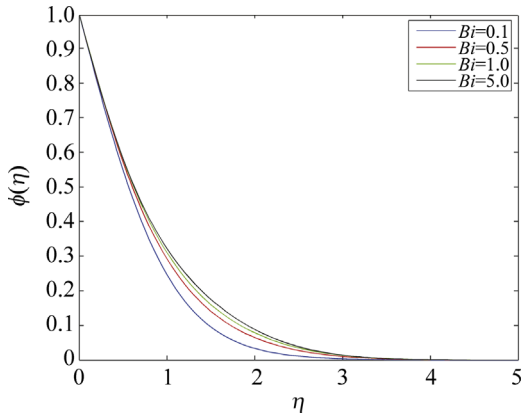

Figure 13 Concentration graph for different values of Bi when $Le=2$, $Nb=Nt=B=0.5$, $A=4$, $M=0.2$, $Pr=\beta=1$.

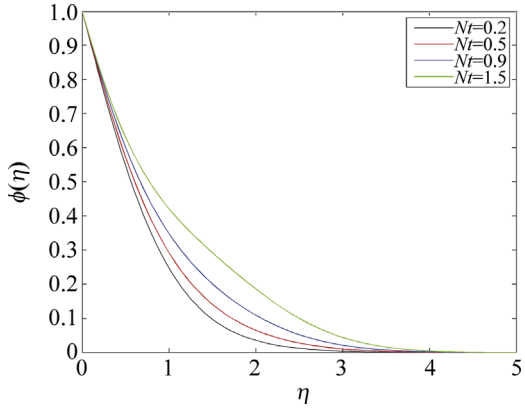

Figure 14 Concentration graph for different values of Nt when $Le=2$, $Nb=Bi=B=0.5$, $A=4$, $Pr=\beta=1$, $M=0.2$.

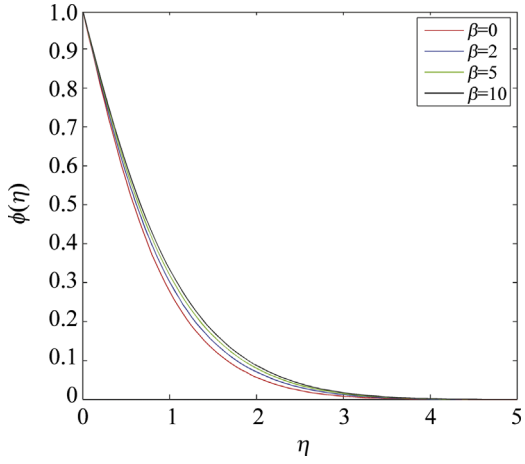

Figure 15 Concentration graph for different values of β when $Le=2$, $Nt=Nb=Bi=B=0.5$, $A=4$, $Pr=1$, $M=0.2$.

Figure 2 demonstrates the variation of velocity graph with respect to magnetic parameter M. As the values of Magnetic parameter M increase, the velocity boundary layer

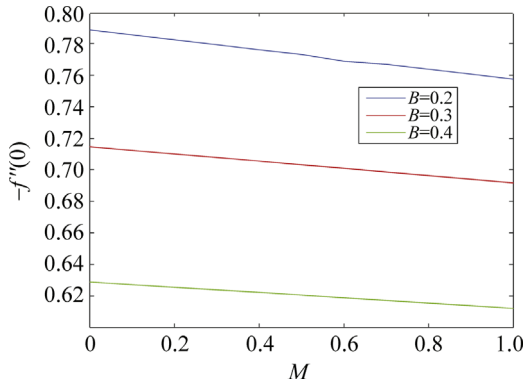

Figure 16 Graph of skin friction coefficient $-f''(0)$ for different values of M along with velocity ratio parameter B when $Le=2$, $Nt=Nb=0.5$, $Pr=1$, $Bi=2$, $A=200$, $\beta=1$.

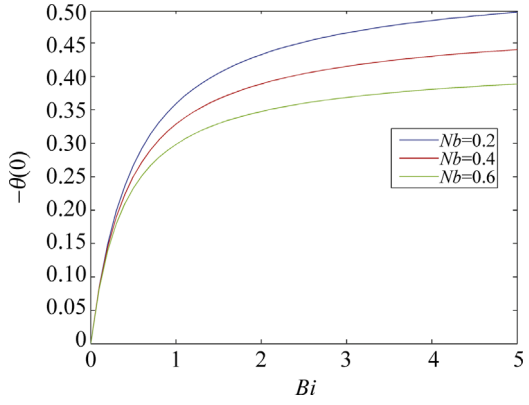

Figure 17 Graph of local Nusselt number $-\theta'(0)$ for different values of Nb when $Le=2$, $Nt=0.5$, $Pr=1$, $A=4$, $B=0.5$, $\beta=0.2$.

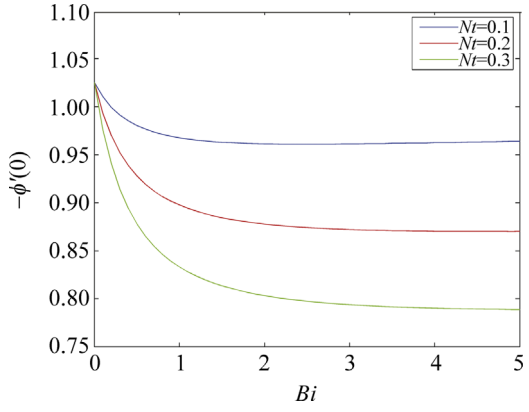

Figure 18 Graph of local Sherwood number $-\phi'(0)$ for different values of Nt when $Nb=0.5$, $Le=2$, $\beta=0.2$, $A=4$, $M=0.2$, $B=0.5$.

thickness increases. This is due to the fact that the presence of transverse magnetic field sets in Lorentz force, which results in retarding force on the velocity field. Therefore, as the values of M increase, so does the retarding force and hence the velocity decreases.

Figure 3 illustrates the influence of Maxwell parameter β on flow velocity. As the values of β decrease, the flow has boundary layer structure and the boundary layer thickness increases as the values of β increase. This is due to the fact that the presence of the non-Newtonian characteristics of viscoelastic flows which decrease the velocity and the boundary layer thickness as well.

Figure 4 illustrates the influence of magnetic parameter M on induced magnetic field graph. As the values of M increase, the graph asymptotically approaches to 1 and the induced magnetic field boundary layer thickness increases when the values of M increase. This is due to the fact that the induced magnetic field and applied magnetic field are in the same direction.

Figure 5 shows the influences of the reciprocal magnetic Prandtl number A on the induced magnetic field. As the values of A increase, the induced magnetic field at the surface increases and the induced magnetic field boundary layer thickness also increases.

Figure 6 elucidates the variation of induced magnetic field as the values of Deborah number β change. As the values of β decrease, the induced magnetic field has a boundary layer structure and its boundary layer thickness increases.

Figures 7–12 represent the variation of temperature with respect to the governing parameters, such as, magnetic parameter M, Biot number parameter Bi, Prandtl number Pr, Deborah number β, Brownian motion parameter Nb and thermophoresis parameter Nt.

Figure 7 depicts the graph of temperature when the value of magnetic parameter M varies. It is found that as the values of M increase, the temperature at the surface and the thermal boundary layer thickness decrease.

Figure 8 shows the effect of Biot number Bi on temperature field. It is found that both the sheet surface and the nanofluid temperature increase when Bi is increased. This leads to an increase in thermal boundary layer thickness. As the value of parameter Bi increases, the intensity of convective heating on the sheet surface increases, which leads to an increasing rate of convective heat transfer from the hot fluid on the lower surface of the sheet to the nanofluid on the upper surface. The graph also reveals that $\theta(\eta)$ increases rapidly near the surface due to the increasing values of Bi.

Figure 9 represents the variation of temperature graph with respect to Prandtl number Pr. The graph depicts that the temperature and thermal boundary thickness decrease when the values of Prandtl number Pr increase at a fixed value of η. This is due to the fact that a higher Prandtl number fluid has relatively low thermal conductivity, which reduces conduction and there by the thermal boundary layer thickness, and as a result, temperature decreases. Increasing Pr is to increase the heat transfer rate at the surface because the temperature gradient at the surface increases. The influence of Prandtl on Newtonian fluids is similar to what we have observed in nanofluid. Therefore, these properties are also inherited by nanofluids.

Figure 10 displays the influence of Deborah number β on temperature profile. As the values of β increase, the thermal

boundary layer thickness also increases. Physically, the Deborah number is the ratio of relaxation time characterizing the time it takes a material to adjust to applied stresses or deformations, and the characteristic time scale of an experiment probing the response of the material. At higher Deborah numbers, the material behavior changes to increasingly dominate by elasticity, demonstrating solid like behavior, thereby slowing down the flow velocity and increasing the temperature of the fluid. Figure 11 represents variation of temperature with respect to Brownian motion parameter *Nb*. As the values of *Nb* increase, the temperature graph is decreasing.

The graph also reveals that the thermal boundary layer thickness increases when the values of *Nb* increase. Moreover, the surface temperature increases as the values of *Nb* increase. The rise in nanofluid temperature can be attributed to nanoparticle interaction linked to increasing Brownian motion.

Figure 12 shows the influence of the change of thermophoresis parameter *Nt* on temperature graph. It can be noticed that as thermophoresis parameter increases, the thermal boundary layer thickness increases but the temperature gradient at the surface decreases (in absolute value) as *Nt* increases. Therefore, the local Nusselt number $-\theta'(0)$, which represents the heat transfer rate at the surface decreases. Consequently, temperature on the surface of a sheet increases.

This is due to the fact that the thermophoresis Parameter *Nt* is directly proportional to the heat transfer coefficient associated to the fluid. The thermal resistance on the hot fluid side is inversely proportional to h_f. Thus, as *Nt* increases, the hot fluid side convection resistance decreases, and as a result, the surface temperature $\theta(0)$ increases.

Figures 13–15 demonstrate the variation of nanoparticle concentration with respect to the change of governing parameters, viz. Lewis number *Le*, Biot number *Bi*, and thermophoresis parameter *Nt*.

It is noticed from Figure 13, as Lewis number increase, the concentration graph decreases. Moreover, the concentration boundary layer thickness decreases as Lewis number increases. This is probably due to the fact that mass transfer rate increases as Lewis number increases. It also reveals that the concentration gradient at surface of the sheet increases.

Figure 14 shows the variation of concentration graph with respect to a change in Biot number *Bi*.

From the graph, it is possible to see that as the values of Biot number parameter *Bi* increase, the concentration graph is decreasing. Moreover, the graph reveals that as the values of *Bi* increase, the concentration boundary layer thickness increases.

Figure 15 shows that as thermophoresis parameter *Nt* increases, the concentration boundary layer thickness also increases. This indicates that an increment in thermophosis parameter induces resistance to the diffusion of mass. This results in the reduction of concentration gradient on the surface.

Figure 16 shows the variation of the skin friction coefficient $-f''(0)$ with respect to *B* as the values of magnetics parameter *M* increases. As the values of *M* increase, the graph decreases and the boundary thickness also decreases.

Table 1 Comparison of skin friction coefficient $-f''(0)$ for different values of velocity ratio parameter *B* when $M=\beta=0$, $Bi=2$.

	Ishak et al. [3]	Ali et al. [9]	Mahapatra and Gupta [2]	Present result
0.1	−0.9694	−0.9694	−0.9694	−0.9694
0.2	−0.9181	−0.9181	−0.9181	−0.9181
0.5	−0.6673	−0.6673	−0.6673	−0.6673
2	2.0175	2.0175	2.0175	2.0175
3	4.7293	4.7293	4.7293	4.7293
5	–	–	–	11.7520
10	–	–	–	36.2574
12	–	–	–	48.2854
15	–	–	–	66.3374

Table 2 Comparison of local Nusselt number $-\theta'(0)$ at $B=M=\beta=0$, $Nt=Nb=10$–12, $Le=2$, $Bi=1000$ for different values of *Pr* with previously published result.

Pr	Makinde and Aziz [27]	Present result
0.2	0.1691	0.1691
0.7	0.4539	0.4539
2	0.9113	0.9113
7	1.8954	1.8954
20	3.3539	3.3539
70	6.4622	6.4622

Table 3 Computed values of skin friction coefficient $-f''(0)$, local Nusselt number $-\theta'(0)$ and local Sherwood number $-\phi'(0)$ for different values of *B*, *M* and *Bi* when $Nb=Nt=0.5$, $Pr=1$, $Le=2$, $A=4$, $\beta=0$.

B	*M*	*Bi*	$-f''(0)$	$-\theta'(0)$	$-\phi'(0)$
0	1	10	0.1521	0.4695	1.0709
0.1			0.1238	0.4676	1.0665
0.2			0.1012	0.4661	1.0629
0.3			0.0827	0.4648	1.0599
0.9			0.0154	0.4601	1.0488
1.5			0.7845	0.5053	1.1546
2			1.8705	0.5529	1.2667
2.4			2.8763	0.5883	1.3504
2	1		1.8705	0.5529	1.2667
	2		1.6746	0.5456	1.2496
	3		1.3683	0.5332	1.2204
	4		0.3744	0.4833	1.1032
		0.1	−0.8626	0.0815	0.9227
		0.5	−0.8626	0.2253	0.8700
		1	−0.8626	0.2845	0.8502
		10	−0.8626	0.3659	0.8251
		20	−0.8626	0.3716	0.8235
		100	−0.8626	0.3761	0.8222

Figure 17 displays the effect of Brownian motion parameter on local Nusselt number against convective parameter Bi. As the values of Bi parameter increase, the graph of local Nusselt number $-\theta'(0)$ increases and the thermal boundary layer thickness also increases.

Figure 18 reveals the effects of thermophoresis parameter Nt on local Sherwood number $-\phi'(0)$ with respect to Bi. As the values of Nt increase, the graph of the local Sherwood number decreases. Furthermore, the concentration boundary layer thickness also decreases.

Table 1 shows the comparison of the variation of skin friction coefficient $-f''(0)$ for different values of velocity ratio parameter B with previous studies. From the table it is possible to see that our result is in an excellent agreement with the results given by researchers [2,3,9] in limiting conditions. Moreover, to check the accuracy of the numerical solutions, a comparison of heat transfer rate for different values of Pr is made with Ali et al. [10] and found an excellent agreement with them.

From Tables 1 and 2, it can be seen that the present result is in an excellent agreement with the results reported by previous studies under limiting conditions. Therefore, the author is confident that numerical method used is suitable for the analysis of the problem.

The variation of $-f''(0)$, $-\theta'(0)$ and $-\phi'(0)$ with respect to velocity ratio B, magnetic parameter M and Biot number Bi is given in Table 3. From the table, it is possible to see that skin friction coefficient decreases when both velocity ratio parameter M and magnetic parameter M increase; however, it remains constant as the values of convective parameter Bi increase. Moreover, the table illustrates that the local Nusselt number -$\theta'(0)$ of the flow field decreases as the values of B and M increase and it increases as the values of Bi increase. It is also indicated that the local Sherwood number $-\phi'(0)$ decreases as the values of all the three parameters increase. However, it remains constant as the values of convective parameter Bi increase. Moreover, the table illustrates that the local Nusselt number $-\theta'(0)$ of the flow field decreases as the values of B and M increase and it increases as the values of Bi increase. It is also indicated that the local Sherwood number $-\phi'(0)$ decreases as the values of all the three parameters increase.

5. Conclusion

A numerical study was presented for a boundary layer and MHD stagnation point flow of upper-convected nanofluid flow over a stretching sheet with induced magnetic field and convective boundary conditions. Using similarity variables, the governing equations were transformed into a set of ordinary differential equations, where numerical solution had been given for different governing parameters. The effects of various governing parameters on the induced magnetic field were examined. The results indicate that the velocity field is sensitive when the Deborah number β is negative and not sensitive when the reciprocal of magnetic Prandtl number is small. Moreover, the velocity graph has shown a change when the velocity ratio is less than or equal to 1. The velocity boundary layer thickness increases as the values of Maxwell parameter β increase.

The induced magnetic field boundary layer thickness decreases as the values of velocity ratio parameter B increase. The inclusion of the effect of Maxwell parameter and induced magnetic field in this study of nanofluid makes this study a novel one. The following conclusions are drawn from the analysis:

1. The thickness of velocity boundary layer decreases with an increase in Deborah number β.
2. The thickness of the induced magnetic field boundary layer increases as the values of Magnetic parameter M increase.
3. The thickness of thermal boundary layer increases with an increase in Biot number and Brownian motion parameters.
4. The thickness of thermal boundary layer decreases as Prandtl number parameter Pr, velocity ratio B and magnetic parameter M increase.
5. The surface temperature $\theta(0)$ increases with an increase in the values of Biot number and Brownian motion; it decreases as the values of Pr and B parameters increase.
6. The thickness of concentration boundary layer increases with an increase in the values of Nt and Bi parameters.
7. The thickness of concentration boundary layer decreases with an increase in Lewis number Le.

References

[1] T.R. Mahapatra, A.S. Gupta, Magnetohydrodynamics stagnation-point flow towards a stretching sheet, Acta Mech. 152 (2001) 191–196.
[2] T.R. Mahapatra, A.S. Gupta, Heat transfer in stagnation point flow towards a stretching sheet, Heat Mass Transf. 38 (2002) 517–521.
[3] A. Ishak, R. Nazar, I. Pop, Mixed convection boundary layers in the stagnation point flow towards a stretching vertical sheet, Meccanica 41 (2006) 509–518.
[4] A. Ishak, K. Jafar, R. Nazar, I. Pop, MHD stagnation point flows towards a stretching sheet, Physica A 388 (2009) 3377–3383.
[5] T.R. Mahapatra, S.K. Nandy, A.S. Gupta, Magnetohydrodynamic stagnation point flow of a power-law fluid towards a stretching sheet, Int. J. Non-Linear Mech. 44 (2009) 124–129.
[6] A. Ishak, N. Bachok, R. Nazar, I. Pop, MHD mixed convection flow near the stagnation point on a vertical permeable surface, Physica A 389 (2010) 40–46.
[7] K.B. Pavlov, Magnetohydrodynamic flow of an incompressible viscous fluid caused by deformation of a plane surface, Magn. Gidrodin. 10 (4) (1974) 146–148.
[8] T. Hayat, M. Qasim, S. Mesloub, MHD flow and heat transfer over permeable stretching sheet with slip conditions, Int. J. Numer. Methods Fluids 66 (2011) 963–975.

[9] F.M. Ali, R. Nazar, N.M. Arifin, I. Pop, MHD boundary layer flow and heat transfer over a stretching sheet with induced magnetic field, Heat Mass Transf. 47 (2011) 155–162.
[10] F.M. Ali, R. Nazar, N.M. Arifin, I. Pop, MHD stagnation point flow and heat transfer towards stretching sheet with induced magnetic field, Appl. Math. Mech. (Engl. Ed.) 32 (4) (2011) 409–418.
[11] F.M. Ali, R. Nazar, N.M. Arifin, I. Pop, MHD mixed convective boundary layer flow towards a stagnation point flow on a vertical surface with induced magnetic field, ASME J. Heat Transf. 133 (2011) 022502 (1–8).
[12] M. Kumari, G. Nath, steady mixed convection stagnation point flow of upper convected Maxwell fluids with induced magnetic field, Int. J. Non-Linear Mech. 44 (2009) 1048–1055.
[13] A. Aziz, Similarity solution for laminar thermal boundary layer over a flat plate with a convective surface boundary condition, Commun. Non-Linear Sci. Numer. Simul. 14 (2009) 1064–1068.
[14] A. Aziz, Hydrodynamic and thermal slip flow boundary layer over a flat plate with constant heat flux boundary condition, Commun. Non-Linear Sci. Numer. Simul. 15 (2010) 573–580.
[15] A. Ishak, A. Yacob, N. Bachok, Radiation effect on the thermal boundary layer flow over a moving plate with convective condition, Meccanica 46 (2011) 795–801.
[16] C. Bataller, Radiation effect for the Blasius and Sakiadis flows with convective surface boundary condition, Appl. Math. Comput. 206 (2008) 832–840.
[17] S. Yao, T. Fang, Y. Zhong, Heat transfer of a generalized stretching/shrinking wall problem with convective boundary condition, Commun. Nonlinear Sci. Numer. Simul. 16 (2011) 752–760.
[18] A. Ishak, Similarity solution for flow and heat transfer over a permeable surface with convective boundary condition, Appl. Math. Comput. 217 (2010) 837–842.
[19] H. Markin, I. Pop, The forced convection flow of a uniform stream over a flat surface with a convective surface boundary condition, Commun. Nonlinear Sci. Numer. Simul. 16 (2011) 3602–3609.
[20] D. Makinde, P. Olanrewaju, Buoyancy Effect on thermal boundary layer over a vertical plate with a convective surface boundary condition, ASME J. Fluids Eng. 132 (2010) 044502 (1-4).
[21] V. Subhashinia, N. Samuela, I. Pop, Effects of buoyancy assisting and opposing flows on mixed convection boundary layer flow over a permeable vertical surface, Int. Commun. Heat Mass Transf. 38 (4) (2011) 499–503.
[22] O. Ajadi, A. Adegoke, A. Aziz, Slip boundary layer flow of non-Newtonian fluid over a flat plate with convective thermal boundary condition, Int. J. Non-Linear Sci. 8 (3) (2009) 300–306.
[23] W.A. Khan, A. Aziz, Natural convection flow of a nanofluid over a vertical plate with uniform surface heat flux, Int. J. Therm. Sci. 50 (2011) 1207–1214.
[24] A.V. Kuznetsov, D.A. Nield, Natural convective boundary-layer flow of a nanofluid past a vertical plate, Int. J. Therm. Sci. 49 (2010) 243–247.
[25] W.A. Khan, I. Pop, Boundary layer flow of a nanofluid past a stretching sheet, Int. J. Heat Mass Transf. 53 (2010) 2477–2483.
[26] A. Yacob, A. Ishak, I. Pop, K. Vajavelu, Boundary layer flow past a stretching/shrinking surface beneath an external uniform shear flow with convective surface boundary condition in a nanofluid, Nanoscale Res. Lett. 6 (314) (2011) 1–7.
[27] O.D. Makinde, A. Aziz, Boundary layer flow of a nanofluid past a stretching sheet with convective boundary condition, Int. J. Therm. Sci. 50 (2011) 1326–1332.
[28] A.M. Olanrewaju, O.D. Makinde, On boundary layer stagnation point flow of a nanofluid over a permeable flat surface with Newtonian heating, Chem. Eng. Comm. 200 (2013) 836–852.
[29] W. Ibrahim, B. Shanker, Boundary-layer flow and heat transfer of nanofluid over a vertical plate with convective surface boundary condition, J. Fluids Eng. – Trans. ASME 134 (2012) 081203 (1–8).
[30] W.A. Khan, R.S. Reddy, Heat and mass transfer in power-law nanofluids over a non-isothermal stretching wall with convective boundary condition, J. Heat Transf. ASME 134 (2013) 112001 (1–7).
[31] K. Vajravelu, K.V. Prasad, L. Jinho, L. Changhoon, I. Pop, A. Robert, V. Gorder, Convective heat transfer in the flow of viscous Ag-water and Cu-water nanofluids over a stretching surface, Int. J. Therm. Sci. 50 (2011) 843–851.
[32] M. Mostafa, T. Hayat, I. Pop, S. Ashar, S. Obaidat, Stagnation point flow of a nanofluid towards a stretching sheet, Int. J. Heat Mass Transf. 54 (2011) 5588–5594.
[33] N. Bachok, A. Ishak, R. Nazar, I. Pop, Flow and heat transfer at a general three-dimensional stagnation point in nanofluid, J. Phys. B 405 (2010) 4914–4918.
[34] W. Ibrahim, B. Shankar, M.M. Mahantesh, MHD stagnation point flow and heat transfer due to nanofluid towards a stretching sheet, Int. J. Heat Mass Transf. 56 (2013) 1–9.
[35] W. Ibrahim, B. Shankar, MHD boundary layer flow and heat transfer of a nanofluid past a permeable stretching sheet with velocity, thermal and solutal slip boundary conditions, J. Comput. Fluids 75 (2013) 1–10.
[36] W. Ibrahim, O.D. Makinde, The effect of double stratification on boundary layer flow and heat transfer of nanofluid over a vertical plate, J. Comput. Fluids 86 (2013) 433–441.
[37] W. Ibrahim, B. Shanker, Magnetohydrodynamic boundary layer flow and heat transfer of a nanofluid over non-isothermal stretching sheet, J. Heat Transf. – Trans. ASME 136 (5) (2014) 051701.
[38] W. Ibrahim, B. Shankar, MHD boundary layer flow and heat transfer due to a nanofluid over an exponentially stretching non-isothermal sheet, J. Nanofluids 4 (1) (2015) 16–27.
[39] W. Ibrahim, Double-diffusive in MHD stagnation point flow and heat transfer of Nano fluid over a stretching sheet, J. Nanofluids 4 (2) (2015) 157–166.
[40] W. Ibrahim, The effect of induced magnetic field and convective boundary condition on MHD stagnation point flow and heat transfer of nanofluid over a stretching sheet, IEEE Trans. Nanotechnol. 14 (1) (2015) 178–186.
[41] W. Ibrahim, O.D. Makinde, MHD stagnation point flow of a power-law nanofluid towards a convectively heated stretching sheet with slip, J. Process Mech. Eng. (2014) (accepted).
[42] W. Ibrahim, O.D. Makinde, Double-diffusive in mixed convection flow of MHD stagnation point Flow and heat transfer due to nanofluid over a stretching vertical sheet, J. Nanofluids 4 (1) (2015) 28–37.
[43] S. Nadeem, R. Ul Haq, Z.H. Khan, Numerical solution of non-newtonian nanofluid flow over a stretching sheet, Appl. Nanosci. 4 (2014) 625–631.

[44] S. Nadeem, R. Ul Haq, Z.H. Khan, MHD three-dimensional boundary layer flow of Casson nanofluid past a linearly stretching sheet with convective boundary condition, IEEE Trans. Nanotechnol. 13 (1) (2014) 109–115.

[45] S. Nadeem, R. Ul Haq, Z.H. Khan, Convective heat transfer and MHD effects on Casson nanofluid flow over a shrinking sheet, J. Cent. Eur. J. Phys. 12 (12) (2014) 862–871.

[46] S. Nadeem, R. Ul Haq, Z.H. Khan, Thermal radiation and slip effects on MHD stagnation point flow of nanofluid over a stretching sheet, Phys. E: Low-Dimens. Syst. Nanostruct. 65 (2015) 17–23.

[47] S. Nadeem, R. Ul Haq, Z.H. Khan, Numerical study of MHD boundary layer flow of a Maxwell fluid past a stretching sheet in the presence of nanoparticles, J. Taiwan Inst. Chem. Eng. 45 (1) (2014) 121–126.